Engineering of Microcrystaline Solid-State Networks Using Cross-Linked γ-Zirconium Phosphate/Hypophosphite with Nonrigid Polyethylenoxadiphosphonates. Easy Access to Porously Dynamic Solids with Polar/Nonpolar Pores

Ernesto Brunet,* María José de la Mata, Hussein M. H. Alhendawi, Carlos Cerro, Marina Alonso, Olga Juanes, and Juan Carlos Rodríguez-Ubis

Departamento de Química Orgánica, Facultad de Ciencias, C-1, Universidad Autónoma de Madrid, 28049-Madrid, Spain

Received July 29, 2004. Revised Manuscript Received November 24, 2004

The construction of organic−inorganic scaffolds based on γ-zirconium phosphate and polyethylenoxa diphosphonates is described. Microcrystalline materials with a controlled, low degree of pillaring are synthesized and characterized by elemental analysis, X-ray powder diffraction, solid-state NMR, and thermogravimetric analysis. The mechanism for the topotactic polyethylenoxa-pillaring reaction is proposed and confronted with previous ones suggested for the reaction of nonpolar organic diphosphonates. The affinity among the polyethylenoxa chains and the superficial acidic phosphates of the layered salt is thus clearly evidenced. The work shows how the inner structure of the pillared microcrystals may be easily modified by a second exchange of the remaining superficial phosphates by other phosphorus species as the low-polar hypophosphite. The rigidity of the layers and the wedge-like effect of intercalated amines at the edges of the microcrystals cause them to increase the interlayer distance, and hence porosity, in a flash fashion.

Introduction

Engineering of crystals[1] and solids is an active area of research that lays a bridge between the concepts of supramolecular chemistry[2] and materials science.[3] The original idea[4] was the design of organic crystals in which the molecules were adequately oriented to suffer topochemical reactions. Yet, modern crystal engineering is synonymous to design principles[5] directed to the synthesis of predefined crystal frameworks with coveted properties and features. There are several methods to shape solid frameworks. Molecular self-assembly[6] is at present one of the most attractive approaches to produce new materials. This assembling is currently established using a number of well-known molecular interactions, that is, metal complexation[7] and hydrogen bonding.[8] The scope of their applications involves quite interesting fields such as optoelectronics,[9] conductivity and superconductivity,[10] charge transfer,[11] magnetism,[12] nano- and biomimetic materials,[13] etc.

The supramolecular construction of nanoporous solids with ample, open voids that can be freely accessed by other molecular species is quite difficult a task pursued by a vast number of research groups.[14] The spontaneous aggregation of dissolved small molecular building blocks is the most common approach (molecular tectonics[15]). However, its success is still rather limited because, for the self-aggregation to render useful architectures, one should possess a profound predictive knowledge of the involved intermolecular forces, which implies the proposition and preparation of effective synthons with suitable geometries and functionalities. Moreover, once the crystal or solid is formed, there are little chances, if any, to further manipulate its structure.[16]

* Corresponding author. E-mail: ernesto.brunet@uam.es.

(1) Desiraju, G. R. *J. Indian Chem. Soc.* **2003**, *80*, 151−155. Desiraju, G. R. *Crystal Engineering: The Design of Organic Solids*; Elsevier: Amsterdam, 1989. Braga, D.; Desiraju, G. R.; Miller, J. S.; Orpen, A. G.; Price, S. L. *CrystEngComm* **2002**, *4*, 500.

(2) Lehn, J. M. *Angew. Chem., Int. Ed. Engl.* **1990**, *29*, 1304. Lehn, J. M. *Supramolecular Chemistry: Concepts and Perspectives*; VCH: Weinheim, 1995.

(3) Desirau, G. R., Ed. *Perspectives in Supramolecular Chemistry. The Crystal as a Supramolecular Entity*; Wiley: Chichester, UK, 1996. Atwood, J. L., Davies, J. E. D., MacNicol, D. D., Voegtle, F., Eds. *Comprehensive Supramolecular Chemistry*; Pergamon: Oxford, 1996; Vol. 11.

(4) Schmidt, G. M. J. *Pure Appl. Chem.* **1971**, *27*, 647.

(5) Hollingsworth, M. D. *Science* **2002**, *295*, 2410−2413. Desiraju, G. R. *Angew. Chem., Int. Ed. Engl.* **1995**, *34*, 2311. Allen, F.; Raithby, P. R.; Shields, G. P.; Taylor, R. *Chem. Commun*. **1998**, 1043.

(6) Lehn, J. M. *Pure Appl. Chem.* **1994**, *66*, 1961.

(7) Moulton, B.; Zaworotko, M. J. *Chem. Rev.* **2001**, *101*, 1629. Chisholm, M. H.; Folting, K.; Huffman, J. C.; Li, H.; Macintosh, A. M.; Wu, D. D. *Polyhedron* **2000**, *19*, 375. Braga, D.; Greponi, F. *Coord. Chem. Rev.* **1999**, *183*, 19.

(8) Desiraju, G. R. *Acc. Chem. Res.* **2002**, *35*, 565. Aakeroy, C. B.; Beatty, A. M. *Aust. J. Chem.* **2001**, *54*, 409. Strauch, H. C.; Rinderknecht, T.; Erker, G.; Frohlich, R.; Wegelius, E.; Zippel, F.; Hoppener, S.; Fuchs, H.; Chi, L. F. *Eur. J. Org. Chem*. **2000**, 187. Ranganathan, A.; Pedireddi, V. R.; Sanjayan, G.; Ganesh, K. N.; Rao, C. N. R. *J. Mol. Struct*. **2000**, *522*, 87.

(9) Marks, T. J.; Ratner, M. A. *Angew. Chem., Int. Ed. Engl.* **1995**, *34*, 155.

(10) Miller, J. S.; Epstein, A. J. *Angew. Chem., Int. Ed. Engl.* **1994**, *33*, 385.

(11) Segura, J. L.; Martin, N. *Angew. Chem., Int. Ed.* **2001**, *40*, 1372. Breu, J.; Kratzer, C.; Yersin, H. *J. Am. Chem. Soc*. **2000**, *122*, 2548.

(12) Gatteschi, D. *Adv. Mater*. **1994**, *6*, 635. Braga, D.; Maini, L.; Prodi, L.; Caneschi, A.; Sessoli, R.; Grepioni, F. *Chem.-Eur. J*. **2000**, *6*, 1310.

(13) Aizemberg, J.; Hanson, J.; Koetzle, T. F.; Weiner, S.; Addadi, L. *J. Am. Chem. Soc*. **1997**, *119*, 881.

(14) DiskinPosner, Y.; Dahal, S.; Goldberg, I. *Angew. Chem., Int. Ed.* **2000**, *39*, 1288. Chen, B. L.; Eddaoudi, M.; Hyde, S. T.; Okeeffe, M.; Yaghi, O. M. *Science* **2001**, *291*, 1021.

(15) Mann, S. *Nature* **1993**, *365*, 499. Simard, M.; Su, D.; Wuest, J. D. *J. Am. Chem. Soc*. **1991**, *113*, 4696.

10.1021/cm048754q CCC: $30.25
Published on Web 02/17/2005

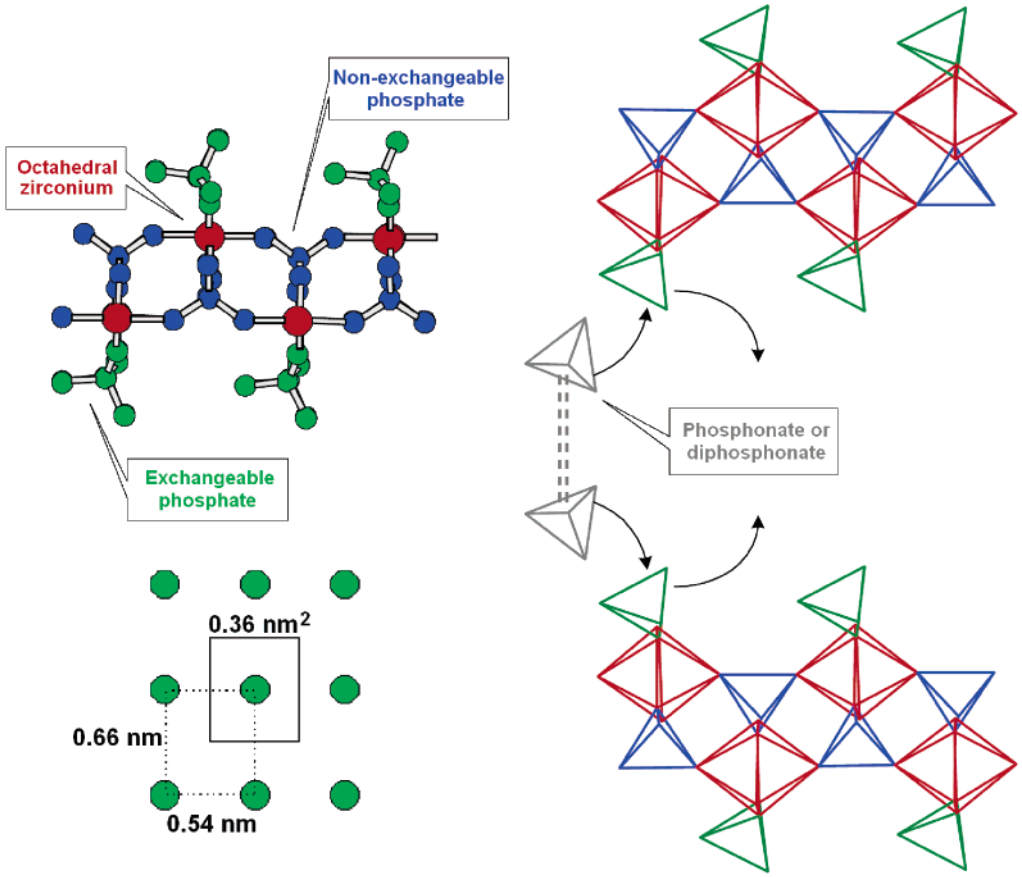

Figure 1. From top left counterclockwise: Schematic structure of a portion of a layer of γ-zirconium phosphate; dimensions of the grid formed by superficial phosphates on a layer; representation of the topotactic exchange of γ-zirconium phosphate by a phosphonate or diphosphonate.

γ-Zirconium phosphate (γ-ZrP) is today a reasonably well-known layered salt[17] in which two different phosphate groups may be distinguished, one bearing all four oxygen atoms bonded to different metal atoms and another one using only two oxygens (Figure 1). The first ones occupy an internal position in the sheetlike structure and maintain its integrity. The other phosphates reside in the surface of the lamellae, forming a grid of ca. 0.55 × 0.65 nm.

These external phosphates can be easily replaced by different oxygenated phosphorus derivatives with at least two oxygen atoms, i.e., phosphonates, without essentially altering the layered estructure.[18] For instance, we have been the first in covalently attaching crown-ether phosphonates to γ-ZrP.[19] The mechanism of the topotactic phosphate/phosphonate exchange has been recently proposed.[20] Organic diphosphonates are then easily attached to opposing faces of different lamellae, leading to pillared, porous solids (Figure 1).[21] Therefore, one can use the well-known layered structure of γ-ZrP as a carving board in which the appropriate organic molecules could be orderly grafted. This fact together with the possibility of exchanging all superficial phosphates remaining from a partial pillaring by other less polar phosphorus functions, that is, hypophosphite,[22] make the prospects of this conceptual combination limited only by the imagination of the researcher. Moreover, by selecting the appropriate functionality of the organic moiety, the resulting material can be reshaped after its preparation by means of simple processes as conformational changes induced by external agents, leading to a phenomenon that could be named supramolecular allostery.[23]

In this paper, we give a full account of our results concerning the low-level pillaring of γ-ZrP with the polyethyleneoxa diphosphonates (**2**) of Scheme 1. We have also prepared the nonpillared γ-ZrP exchanged phases with the corresponding monophosphonates (**3**) for comparison purposes.

Quite interestingly, the polyethyleneoxa chains of the created materials showed a high affinity for the phosphate surface. This affinity could be gradually disrupted by simple acid−base reactions, the intercalated base acting as effective wedges that increase the interlayer spacing. This effect[24] was revealed to be exceedingly sensitive to tiny pH changes when the superficial phosphates were replaced by hypophosphite.[25]

(16) For a recent, excellent example, see: Saied, O.; Maris, T.; Wuest, J. D. *J. Am. Chem. Soc.* **2003**, *125*, 14956.
(17) Clearfield, A.; Poojary, D. M. *J. Chem. Soc., Dalton Trans.* **1995**, 111.
(18) For pioneering work, see: Yamanaka, S.; Hattori, M. *Inorg. Chem.* **1981**, *20*, 1929. Clearfield, A.; Ortiz-Ávila, C. Y. *Inorg. Chem.* **1985**, *24*, 1773.
(19) Brunet, E.; Huelva, M.; Rodríguez-Ubis, J. C. *Tetrahedron Lett.* **1994**, *35*, 8697. Brunet, E.; Huelva, M.; Vázquez, R.; Juanes, O.; Rodríguez-Ubis, J. C. *Chem.-Eur. J.* **1996**, *2*, 1578. See also: Alberti, G.; Boccali, L.; Dionigi, C.; Vivani, R.; Kalchenko, V. I.; Atamas, L. I. *Supramol. Chem.* **1996**, *7*, 129.
(20) Alberti, G.; Giontella, E.; Murcia-Mascarós, S. *Inorg. Chem.* **1997**, *36*, 2844.
(21) Alberti, G.; Costantino, U.; Marmottini, F.; Vivani, R.; Zappelli, P. *Angew. Chem., Int. Ed. Engl.* **1993**, *32*, 1357.
(22) Alberti, G.; Casciola, M.; Biswas, R. K. *Inorg. Chim. Acta* **1992**, *201*, 207.
(23) Brunet, E.; Juanes, O.; Mata, M. J.; Rodríguez-Ubis, J. C. *Eur. J. Org. Chem.* **2000**, 1913.

Scheme 1. Phosphonic Acids Synthesized in This Work (n = 1−5)

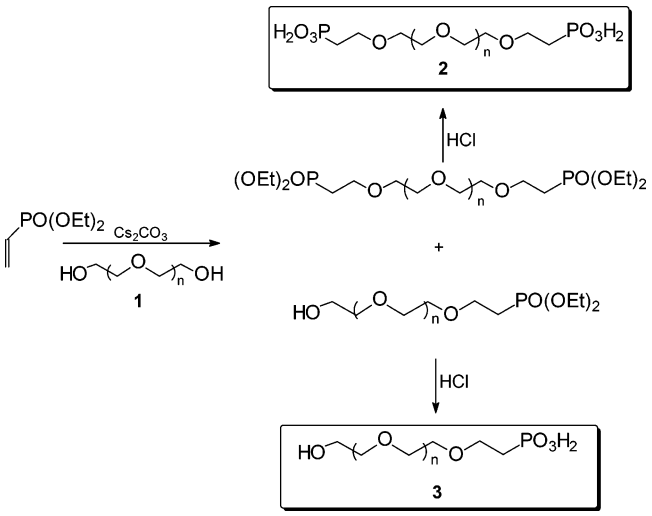

Therefore, (i) the length of the organic chain, (ii) the polarity of the layer surface, and (iii) the pH can finely tune the size and shape of the void spaces in the resulting insoluble solid. To our knowledge, this is the first full report in which the porosity of a microcrystalline solid can a priori be controlled by the selection of organic chains of different length and a posteriori by simple acid−base reactions.[26]

Experimental Section

All commercial reagents were purchased from Aldrich or Fluka and used as received. Solution ^{1}H, ^{13}C, and ^{31}P NMR spectra were recorded on either a Bruker AC-200 or a AC-300 instrument. Solid-state ^{31}P NMR spectra were recorded under MAS and CP-MAS techniques on a Bruker MSL-400 instrument. MS L-SIMS spectra were recorded on a VG AutoSpec spectrometer. X-ray powder diffraction spectra were recorded at room temperature on either Phillips PW1710 or Siemens D-5000 diffractometers with Cu Kα radiation and Ni filter (40 kV, 30 mA). Thermogravimetric analysis was performed on a Mettler-Toledo TGA/STDA 851e apparatus and recorded at 5 °C/min. Structure modeling was carried out on PC computers using the Hyperchem 6.0 and 7.5 software. Synthetic procedures and spectroscopy data are included as Supporting Information.

Results and Discussion

Topotactic Reaction. Table 1 shows the results of the topotactic pillaring with the studied compounds **2** (Scheme 1) in various conditions.

MAS ^{31}P NMR solid-state spectra of the materials showed the expected signals for the γ-ZrP phosphates at −27.2 (internal PO_4) and −13.6 ppm (superficial H_2PO_4) and the exchanged phosphonates at 17−20 ppm. Provided a long relaxation delay (>10 s) was given, the relative signal areas were in excellent agreement with the exchange levels deduced from elemental analyses and solution ^{31}P NMR spectra in HF/DMSO-d_6. The TGA curve (Supporting Information) for **H25** is typical of those observed for all prepared materials. Four clear weight transitions are observed in all cases at the indicated temperature intervals, the most revealing ones being the loss of water (25−150 °C) and the organic component (150−350 °C). The latter has been assigned to elimination of glycol fragments and is in all cases in very good agreement with the exchange levels measured by elemental analysis and NMR measurements. A complete account of the thermal degradation of these materials will be published elsewhere.

There are two features in Table 1 that should be remarked. The first feature is the maximum level of exchange ($2x$ in the empirical formula $Zr_{100}(PO_4)_{100}(H_2PO_4)_{100-2x}[C_6H_{16}O_8P_2(C_2H_4O)_n]_x\cdot(H_2O)_z$), which is summarized in Figure 2. The figure also contains the exchange of γ-ZrP with 1,10-decendiphosphonate performed by us from literature data[27] for comparison purposes. It can be seen that, while exchange levels close to 100% were easily reached for the nonpolar 1,10-decendiphosphonate without the need of an excess of reactant (circles), large molar excesses of diphosphonates **2** per zirconium are required to reach relatively low exchange levels of up to 60−70%. The 0.66 × 0.54 nm rectangular networks (cf. Figure 1) formed by superficial phosphates in γ-ZrP leave an accessible area of 0.36 nm^2 for an organic chain once the topotactic exchange takes place. Simple modeling indicates that this space should be more than enough to accommodate the cross section of simple organic chains as those of linear alkyl or polyethylenoxa groups. However, only the diphosphonates derived from the latter displayed serious difficulties in attaining high exchange values.

The second feature to be highlighted concerns interlayer distances, which appeared to be nearly independent of the length of the exchanged **2**. The conditioned materials over $BaCl_2$ (90% r.h.) showed almost a constant interlayer separation of ca. 1.35 nm (cf. Table 1), very different from that observed for the pillared material with 1,*n*-alkyldiphosphonates. When the material was put in good contact with water (stirred in water, centrifuged, and the slurry directly placed in the X-ray diffractometer), the interlayer distance only increased to an average of 1.80 nm, still much shorter than the expected value for the pillared materials. Molecular modeling of the zigzag and helicoidal conformations of the polyethylenoxa diphosphonates predicted height cross sections of 0.3 and 0.7 nm, respectively, for the molecules resting longitudinally. Taking into account that the thickness of a γ-ZrP layer is 0.95 nm, the measured average interlayer distances of 1.35 nm (conditioned) and 1.80 nm (wet) indicate that the polyoxa chains remain in an almost parallel arrangement relative to the lamellae, regardless of the amount of water present.

(24) In a previous paper, we designated the change in interlayer spacing induced by solvent intercalation or acid−base titrations as an accordion-like effect (Alberti, G.; Brunet, E.; Dionigi, C.; Juanes, O.; Mata, M. J.; Rodríguez-Ubis, J. C.; Vivani, R. *Angew. Chem., Int. Ed.* **1999**, *38*, 3351). We now find this conceptual image as somewhat improper because the layers most probably slide relative to one another and the pillars do not shrink but incline. For an excellent review on this topic, see: Clearfield, A.; Wang, Z. *J. Chem. Soc., Dalton Trans.* **2002**, 2937.

(25) Brunet, E.; Mata, M. J.; Juanes, O.; Rodríguez-Ubis, J. C. *Angew. Chem., Int. Ed.* **2003**, *42*, 3714.

(26) For an example of postsynthesis modification of the chemical structure, not porosity, of a porous zirconium phosphonate, see: Wang, Z.; Heising, J. M.; Clearfield, A. *J. Am. Chem. Soc.* **2003**, *125*, 10375.

(27) Alberti, G.; Murcia-Mascarós, S.; Vivani, R. *J. Am. Chem. Soc.* **1998**, *120*, 9291.

Table 1. Results of the Topotactic Pillaring of γ-ZrP with the Diphosphonic Acids 2 of Scheme 1

2 atoms(n)[a]	equiv acid/Zr	[acid] (mM)	x[b]	z[c]	condit.	d[d] wet	calc.	material acronym[e]
11(1)	0.4	15	13	130	1.31	1.57	2.0	D25
	3.0	50	28	140	1.37	1.64		D55
	5.9	100	33	130	1.49	1.61		D70
14(2)	0.4	15	12	125	1.31	1.61	2.3	Ti25
	3.2	75	22	90	1.32	1.64		Ti50
17(3)	0.4	15	15	100	1.31	1.73	2.6	Te25
20(4)	0.4	15	13	80	1.31	1.76	2.9	P25
	3.5	100	32	60	1.32	2.28		P65
23(5)	0.4	15	12	90	1.37	1.76	3.2	H25
	3.5	100	29	30	1.88	2.05		H60

[a] See Scheme 1 and empirical formula: $Zr_{100}(PO_4)_{100}(H_2PO_4)_{100-2x}[C_6H_{16}O_8P_2(C_2H_4O)_n]_x\cdot(H_2O)_z$. [b] Exchange level deduced from elemental analysis and liquid ^{31}P NMR in HF/DMSO-d_6. [c] Water content determined by TGA and elemental analysis in conditioned samples. [d] Powder XRD interlayer distance (nm) measured in conditioned samples over $BaCl_2$ (90% r.h.) or just after centrifugation (wet); expected interlayer distance (calc) for the exchanged γ-ZrP with alkyl 1,m-diphosphonate having the same number of atoms as the corresponding polyethyleneoxa chain. [e] Letters indicate the polyethylenglycol precursor of the polyethylenoxa diphosphonate (Scheme 1); numbers indicate the level of exchange [i.e., **P25** means γ-ZrP exchanged ca. 25% with **2** (n = 4)].

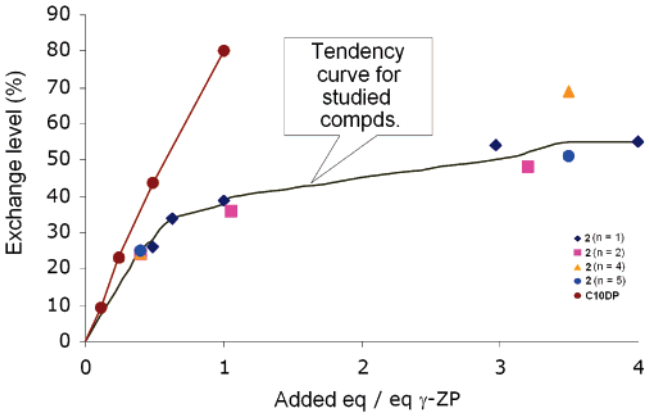

Figure 2. Plot of the achieved exchange level versus the amount of added equivalents (referred to Zr) of diphosphonic acids **2** of Scheme 1 and 1,-10-decendiphosphonic acid (**C10DP**; terracotta circles).

There is a third fact not indicated in Table 1 that concerns flocculation times of the cross-linking process, the reaction of γ-ZrP with compounds **2** being much faster (ca. 10 min) than that of the 1,n-alkyldiphosphonates (several hours).

In summary, polyethylenoxa diphosphonates led to (i) low topotactic exchange levels even with high concentrations of the organic component; (ii) no heavy swelling of the polyethylenoxa-pillared materials in the presence of water; and (iii) very short flocculation times to isolate the solid material. This behavior suggests a strong interaction, probably by hydrogen bonding, between the ethylenpolyoxa chains and the acid phosphates in the surface of the inorganic layer. This made us think that the mechanism of the topotactic exchange of the polar polyethylenoxa diphosphonates should be somewhat different from that of nonpolar analogues. Figures 3 and 4 summarize our proposal.

By resemblance to the pillaring reaction of γ-ZrP with rigid diphosphonic acids,[28] the exchange process of an alkyldiphosphonate should occur in various steps (Figure 3).

First, the exfoliated lamellae (A), colloidally dispersed in water−acetone at 80 °C, quickly admit the incorporation of a layer of diphosphonic acid (B),[29] the latter acting as a monovalent anionic ligand. The alkyl chains, with no affinity to the polar phosphate layer, should remain in a mostly perpendicular-to-the-lamellae zigzag arrangement (B). It then looks plausible that the derivatized γ-ZrP lamellae start interacting in a way similar to a lipid membrane (C). Interdigitation of the alkyl chains is then needed to form the truly pillared material (D). A sluggish interdigitation process might provide a good explanation for the slowness in the flocculation of the alkyldiphosphonate-containing γ-ZrP.

In the case of our polyethylenoxa diphosphonic acids **2** (Figure 4), the mechanism should be similar but the oxygen present in the organic chains should force the latter to lie parallel to the lamellae (G). The affinity among the phosphates and the polyethylenoxa chains hampers further integration of new phosphonates, thus making the incorporation of **2** a substrate-inhibited reaction. This fact explains the difficulties in attaining high exchange levels. Yet, two different layers can be in close contact much more easily (H) because the interdigitation step is no longer necessary, and therefore flocculation may occur at a faster pace but with a lower overall exchange rate.

We are aware that this mechanism may raise questions about the true pillared nature of the **2**-exchanged γ-ZrP materials, because in step G (Figure 4) the reaction of the second phosphorus group of the diphosphonate might take place in the same layer, thus forming loops as shown in Figure 5.

Before solving this problem, we should mention that it is well established by IR studies that polyethylenglycols adopt helicoidal conformations in water. All of our pillared materials (conditioned or wet) displayed the wagging (1353−1355 cm^{-1}) and torsion (1305−1307 cm^{-1}) bands attributed in the literature to $O-CH_2-CH_2-O$ fragments in gauche conformation,[30] necessary for the polyethylenoxa chains to adopt helicoidal arrangements.

Figure 6 illustrates the key experiment, the outcome of which completely rules out the forming of loops, ensures the truly pillared character of our materials, and is fully

(28) Alberti, G.; Giontella, E.; Murcia-Mascarós, S.; Vivani, R. *Inorg. Chem.* **1998**, *37*, 4672.

(29) We have modeled the attachment of diphosphonates to the opposing faces of two consecutive lamellae for the sake of clarity. The whole process should obviously involve the carpeting of all faces of the exfoliated lamellae and the piling of a certain number of layers leading to typically sized particles (Coulter method, 0.5−2 μm).

(30) Begum, R.; Matsuura, H. *J. Chem. Soc., Faraday Trans.* **1997**, *93*, 3839.

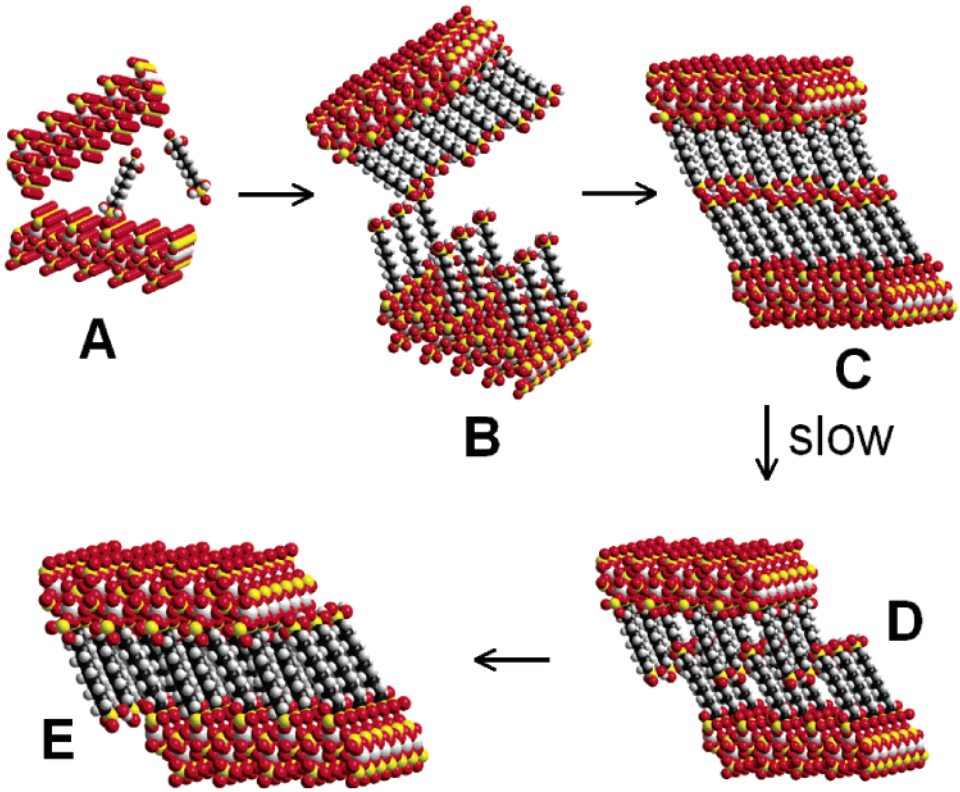

Figure 3. Schematic proposal for the mechanism of the topotactic exchange of γ-ZrP with 1,10-decendiphosphonic acid (see ref 29).

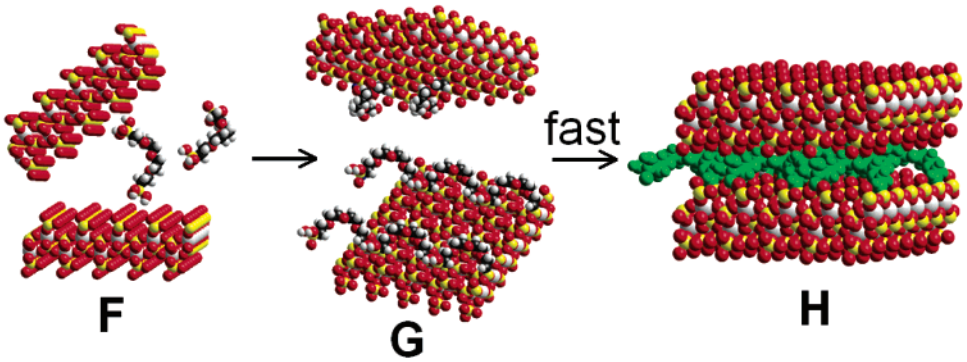

Figure 4. Schematic proposal for the mechanism of the topotactic exchange of γ-ZrP with **2** ($n = 1$; see Scheme 1 and ref 29).

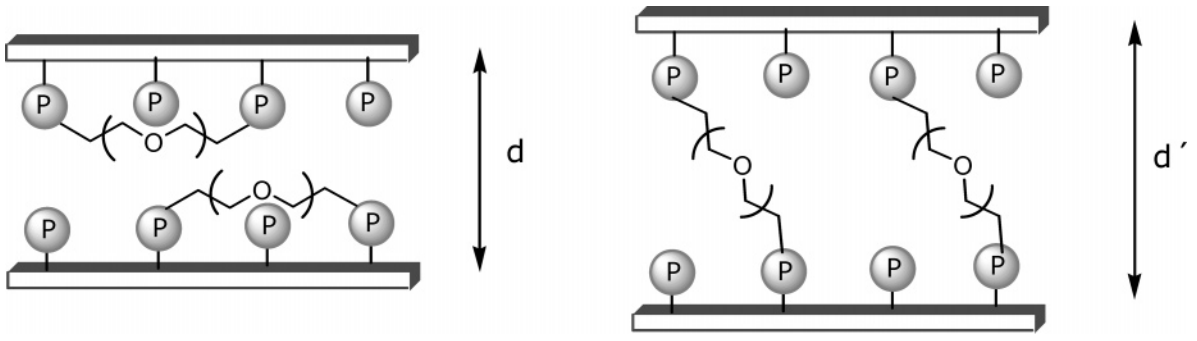

Figure 5. Possible arrangement of polyethylenoxa chains forming loops (left) or true pillars (right).

consistent with the helicity of the polyethylenoxa chains hinted by IR data.

The materials bearing phosphonate/phosphate exchange levels of ca. 25% ($x = 12-15$ in Table 1) were titrated up to pH = 9 with methylamine, and the interlayer distances of the resulting wet, neutralized materials were measured by powder XRD analysis (triangles in Figure 6). It can be seen that the measured basal spacings are in excellent agreement with those calculated by molecular modeling for a helicoidal conformation of the polyethylenoxa chain. Moreover, when γ-ZrP was exchanged with the corresponding monophosphonates (**3** in Scheme 1; their structure with a single phosphorus end makes the formation of pillars impossible) and the resulting materials were titrated with

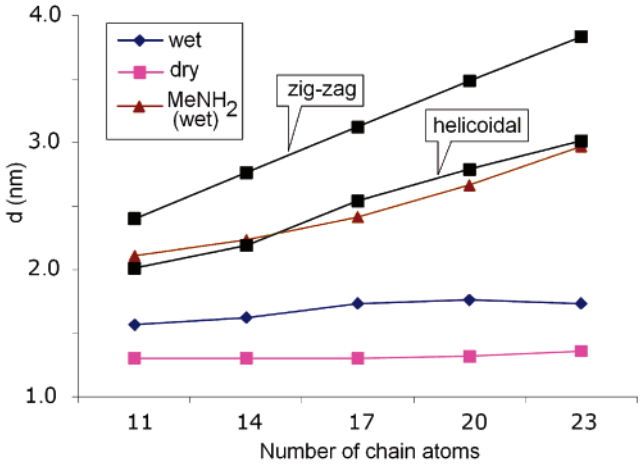

Figure 6. Interlayer distances of γ-ZrP phases pillared at 25% level with the studied polyethylenoxa diphosphonic acids (Scheme 1) in dry (pink ■) and wet (◆) conditions and intercalated with methylamine (▲). The figure also contains calculated interlayer distances (■) for the indicated conformations of the polyethylenoxa pillars.

methylamine in the same conditions, an amorphous solid was formed as shown by the absence of peaks in powder XRD spectra.

These relatively simple experimental considerations make us conclude that the exchange of γ-ZrP with polyethylenoxa diphosphonates **2** provides an easy access to building porous pillared materials whose final porosity can be tuned by the topotactic exchange reaction itself and is dramatically varied by the acid−base intercalation of simple species.

Figure 7 shows the evolution of interlayer distance of **D25** and **P25** with the increasing amount of methylamine. The behavior of the two materials is notoriously different. The material with the short polyethylenoxa chain (**D25**) needs 0.5 equiv of amine to start increasing interlayer distance, whereas that with the larger chain (**P25**) starts swelling from the very beginning the amine was added. In our belief, this is another evidence of the existence of an intricate hydrogen-bonding network among the nonexchanged exchangeable phosphates and the polyethylenoxa chains.

The ca. 25% level of phosphate/phosphonate exchange attained in materials **D25** and **P25** means that there are approximately 12 polyethylenglycol chains for every 76 phosphates. On the other hand, **D25** and **P25** have, respectively, three and six oxygen atoms in their chains (cf. Scheme 1 and Table 1). One may realize by this simple consideration that the number of chain oxygen atoms in **P25** almost equals that of its remaining exchangeable phosphates, which gives the possibility of nearly all of them being involved in hydrogen bonding. A small amount of methylamine should be enough to start disrupting the hydrogen-bonding network that glues the lamellae, thus making the interlayer distance quickly increase with the first amine additions. On the contrary, in **D25**, the amount of chain oxygen atoms is one-half of that of **P25**, and at least ca. 50% of the phosphates cannot be involved in hydrogen bonding. The first 0.5 equiv of amine can thus diffuse into the interlayer space and react with the acidic phosphates without affecting hydrogen bonding with the organic chains. The initial interlayer distance can be thus maintained in **D25** along the first additions of methylamine.

When one OH of all acidic phosphates has been neutralized with methylamine, hydrogen bonding seems to be no longer possible and the polyethylenoxa chains stand up. It should be remarked that at this point the wagging band (1353−1355 cm^{-1}) attributable to $O-CH_2-CH_2-O$ fragments in gauche conformation is still clearly visible. We thus assume the polyethylenoxa chains to be helicoidally arranged. Interlayer distances calculated by molecular modeling are in excellent agreement with this assumption (cf. Figure 6). TGA indicates a water content per molecular formula (z in Table 1) of 100 and 385, respectively, for conditioned samples of **D25** and **P25** titrated with methylamine to pH = 9, meaning that the large pores created in the material with the longest organic chain are filled with additional water molecules.

We have explored whether these large pores can include other simple molecules different from water, that is, alkylamines of various lengths. The simple intercalation of alkylamines into γ-ZrP has been widely studied and it is well known that the amines arrange as a double layer, the longitudinal mean axis of their zigzag conformation forming an angle of 50° with the layer planes.[31] The interlayer distance (d) increases linearly following the relationship $d = 1.08 + 0.19n$, where n is the number of carbons of the alkylamine (Figure 8). However, using **Te25** for this test, we have obtained the sigmoid curve shown in Figure 8 for the intercalation of methyl-, hexyl-, decyl-, dodecyl-, tetradecyl-, and octadecylamine.

In all cases, elemental analysis, NMR, and TGA studies indicate an incorporation of ca. 70−80% of amine, which approximately corresponds to one amine molecule per nonexchanged superficial phosphate. The sigmoid curve displayed by **Te25** implies a reluctance of this pillared material to increase interlayer distance, as compared to plain γ-ZrP, which is especially notorious at the starting and ending plateaus, hence with both the shortest and the longest amines. The case of the short amines should be another manifestation of the affinity of the chains for the γ-ZrP surface, and that of the largest ones should be a manifestation of the difficulty in the elongation of the pillars.

The two dashed lines indicate the maximum calculated interlayer distances by molecular modeling for **Te25** when the ethylenepolyoxa chains are as perpendicular as possible to the layers in helicoidal (ca. 2.5 nm) and zigzag (ca. 3.2 nm) arrangements. The variation of interlayer distance from hexyl- to tetradecylamine, that crosses the predicted interlayer distance for the helicoidal arrangement of the columns, follows the equation $d = 1.08 + 0.16n$. The smaller slope displayed by the pillared material (0.16) as compared to plain γ-ZrP (0.19) means that the angle of the amines with respect to the layer planes has to be 10° lower than in the absence of polyethylenoxa pillars. Despite that, the columns appear to show enough conformational mobility to allow for the intercalation of even longer alkylamines. In the case of octadecylamine, the interlayer distance seems to reach a limit, very close to the maximum predicted by the models for the

(31) See, for example: Costantino, U.; Clearfield, A. In *Comprehensive Supramolecular Chemistry*; Alberti, G., Bein, T., Eds.; Pergamon Press: New York, 1996; Vol. 7, Chapter 4.

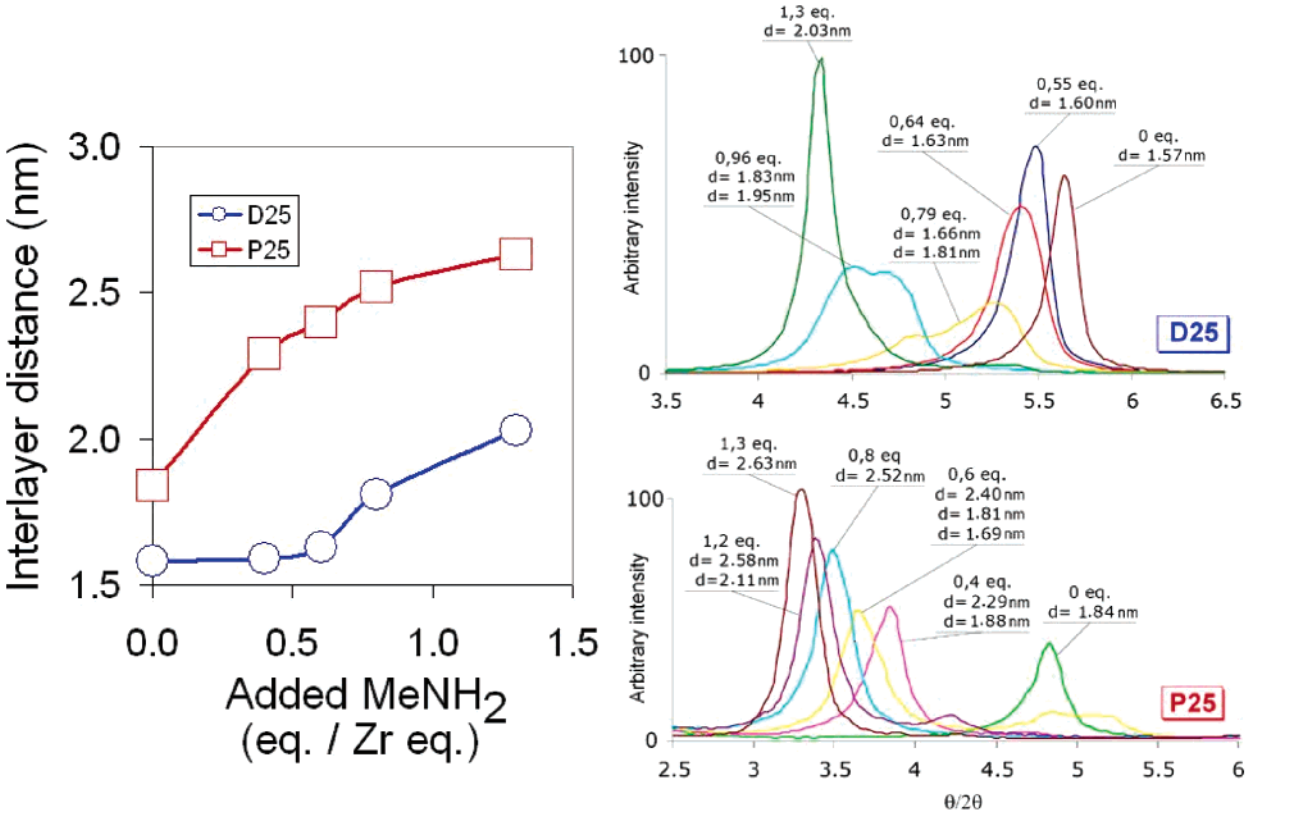

Figure 7. Variation of interlayer distance of the indicated materials with the amount of added methylamine. The insets show expansions of the corresponding X-ray powder patterns at the indicated amine additions.

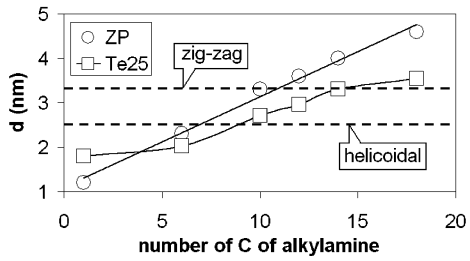

Figure 8. Variation of interlayer distance in conditioned samples of γ-ZrP (literature data) and **Te25** intercalated with methyl-, hexyl-, decyl-, dodecyl-, tetradecyl-, and octadecylamine.

polyethylenoxa column to be in an all-anti zigzag arrangement. The space left between the layers makes the alkyl chain of octadecylamine bow even further, its angle with respect to the layer plane being reduced to 35°. This behavior hints to a possible length and shape selectivity of our pillared materials toward intercalation of amines[32] and other compounds. Besides, the experimental evidence gathered in this work that points to the helicity of the polyethylenoxa columns introduces the idea of achieving supramolecular chirality, provided we devise a method to select their P or M arrangement. These issues are the subjects of upcoming experiments.[33]

Double Exchange with Hypophosphite. In previous work, we observed that the material resulting from the γ-ZrP exchange with an organic phosphonate is amenable of a second exchange with another suitable phosphorus derivative.[34,35] Therefore, the polar phosphates of the layer surface might be easily replaced by less polar phosphorus derivatives. This versatility gives full access to the meccano game depicted in Scheme 2.

Scheme 2. Combination of Porous/Nonporous Pillared Materials Studied in This Work

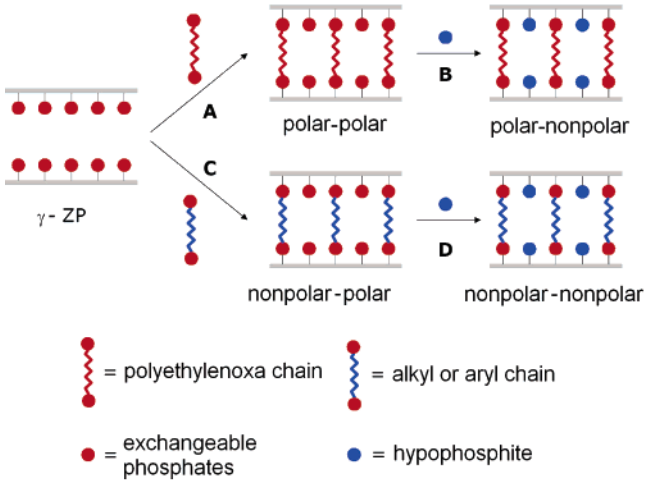

Starting from γ-ZrP, route A leads to the materials described above, where the organic chain is as polar as that of polyethylenoxa diphosphonates **2**. From these materials, the remaining exchangeable phosphates will be further replaced by hypophosphite (route B), leading to new materi-

(32) Tsuyoshi, K.; Shinichi, W.; Kaoru, O.; Masato, M. *Chem. Commun.* **1995**, 75.
(33) Brunet, E. *Chirality* **2002**, *14*, 135.
(34) Brunet, E.; Huelva, M.; Vázquez, R.; Juanes, O.; Rodríguez-Ubis, J. C. *Chem.-Eur. J.* **1996**, *2*, 1578.
(35) Brunet, E.; Alonso, M.; Mata, M. J.; Fernández, S.; Juanes, O.; Chavanes, O.; Rodríguez-Ubis, J. C. *Chem. Mater.* **2003**, *15*, 1232.

Table 2. Results of the Double Exchange with Hypophosphite of P25 Phase in Various Conditions

entry	equiv hypo./Zr	[acid] (M)	x^a	y^a	z^a	d^b wet/cond./dried	material acronym[c]
1	0.25	0.01	12	20	110	1.69/1.30/1.29	P25H20
2	1−2	0.05−0.1	12	42	80	1.28/1.28/1.28	P25H40
3[d]	30	1	14	65	60	1.28/1.26/1.26	P25H65
4[e]	30	1	31	38	100	1.28/1.27/1.26	P60H40
5	120	4	10	70	60	1.27/1.27/1.27	P20H70
6[f]	30	1	13	74	70	1.27/1.26/1.25	P25H75

[a] Empirical formula: $Zr_{100}(PO_4)_{100}(H_2PO_4)_{100-2x-y}(H_2PO_2)_y[C_6H_{16}O_8P_2(C_2H_4O)_4]_x \cdot (H_2O)_z$; exchange level deduced from elemental analysis and liquid ^{31}P NMR in HF/DMSO-d_6; water content determined by TGA and elemental analysis in conditioned samples. [b] Powder XRD interlayer distance (nm) of samples wet/conditioned over $BaCl_2$ (90% r.h.)/dried at 100 °C. [c] **P** stands for γ-ZrP exchanged with **2** ($n = 4$; cf. Scheme 1), **H** for hypophosphite, and numbers indicate the respective levels of exchange (i.e., **P25H20** means 25% exchanged γ-ZrP with **2** ($n = 4$) doubly exchanged with ca. 20% hypophosphite). [d] A small amount of **2** ($n = 4$; 0.10 equiv/Zr) was added to prevent diphosphonate losses. [e] As in previous footnote: added **2** ($n = 4$; 0.40 equiv/Zr). [f] Starting phase **P25** previously treated with methylamine to pH = 7 (see text).

als where the surface of the layers will be turned to nonpolar. We complete this road map to all possible combinations of polar/nonpolar columns and surfaces by the double exchange with hypophosphite (route D) of γ-ZrP already containing nonpolar alkyl- or aryldiphosphonates (route C), but these results will be the subject of future papers.

We selected **P25** as the starting material to perform double exchange with hypophosphite (route B). Table 2 summarizes the results of the different experiments. After various attempts (entries 1, 2, 5) using increasing amounts of hypophosphite (up to 120 times that of Zr and concentrations up to 4 M), NMR experiments and elemental analysis revealed that 10−20% of exchangeable phosphates still remained intact. Losses of polyethylenoxa diphosphonate became important only at the highest hypophosphite concentration. The addition of a small amount of **2** ($n = 4$; cf. Scheme 1) to the reaction mixture (entry 3) avoided this problem, but total hypophosphite incorporation was still unseen. To this effect, entry 4 should be highlighted. When only 0.4 equiv/Zr of **2** ($n = 4$) was added to the excess of hypophosphite in the typical exchange conditions (see Experimental Section), the starting **P25** ended up in **P60H40**, a material whose analytical data indicated an unexpected high **2** ($n = 4$) content (60% exchange). It should be recalled that, beginning with plain γ-ZrP, this level of exchange had to be achieved by using a 4 times molar excess of **2** ($n = 4$) (cf. Table 1 and Figure 2). It looks plausible that at the very moment the majority of the exchangeable phosphates have been replaced by the less polar hypophosphite, the polyethylenoxa pillars no longer have affinity to the surface and the material swells. The small amount of the added diphosphonate is thus allowed to entirely diffuse into the interlayer region. The final outcome is the incorporation of practically all supplementary diphosphonate, suggesting that some of the hypophosphites that just replaced the superficial phosphates were further substituted by phosphonates. Taking into account that the hypophosphites are easily oxidized to phosphates at high pH (see below), lowering the polarity of the surfaces of a γ-ZrP phase containing a low level of polar columns by a second hypophosphite exchange, in the presence of the diphosphonate pillars, may constitute the strategy of choice to high pillaring without using a large excess of the polar organic moiety.

The difficulties in replacing all superficial phosphates by hypophosphite must come in the first place by the fact that the organic columns obviously prevent exfoliation in water/acetone 1:1 at 80 °C. Moreover, the demonstrated affinity of the polyethylenoxa chains by the γ-ZrP surface must thwart swelling in the conditions of hypophosphite exchange, and hydrogen-bonding interactions protect some of the acidic phosphates, making their total replacement impossible at reasonable hypophosphite concentrations.

Because amine intercalation effectively breaks off the hydrogen-bonding network (see above), we finally succeeded in smoothly replacing all phosphates treating first **P25** with methylamine to pH = 7. In those conditions, the pillared material is successfully swelled and hypophosphite is thus free to diffuse between the layers and replace all phosphates, leading to a new material (**P25H75**) with low pillaring. Elemental analysis and TGA gave $Zr(PO_4)(H_2PO_2)_{0.74}(C_{14}H_{30}P_2O_{12})_{0.13} \cdot 0.8H_2O$ as the empirical formula for **P25H75**. A sample of this material, dissolved in HF/D_2O, gave a ^1H NMR spectrum with signals at 0.0, 8.9, and 25.3 ppm attributable to phosphoric, hypophosphorus, and phosphonic acids, respectively. Their relative intensity (3.97:2.91:1) was in excellent agreement with the calculated value (3.84:2.85:1) for the empirical formula obtained from the other techniques. IR of **P25H75** showed the expected stretching P−H band at 2403 cm^{-1}, while solid-state MAS ^{31}P NMR revealed the presence of the internal phosphates at −27.9 and the complete disappearance of the signal at −13.6 ppm belonging in the starting material **P25** to the remaining surface phosphates. Both hypophosphite and phosphonate groups gave at ca. 10 ppm a broad signal, whose intensity heavily increased under CP conditions. Powder XRD of **P25H75** showed a reasonable degree of crystallinity and a very short interlayer distance of 1.28 nm, which was independent of the degree of humidity of the sample.

The forces governing layer piling in γ-ZrP and γ-ZrP/hypophosphite (γ-ZrPH) salts should be very dissimilar. In γ-ZrP, water molecules are sandwiched between the layers, aiding in the formation of a network of strong hydrogen-bonding interactions. In appropriate conditions of polarity and temperature (1:1 water−acetone, 80 °C), the hydrogen-bonding net is broken and γ-ZrP exfoliates, each lamella being effectively solvated. Yet, the γ-ZrPH phase lacks the superficial phosphates and the layer surfaces are carpeted by a grid of nonpolar PH_2 bonds that glue the lamellae to one another by sturdy hydrophobic, van der Waals forces. Therefore, the γ-ZrPH phase is very compact (interlayer distance of 0.88 nm) and cannot be exfoliated in water or any other solvent. Besides, the very low acidic character of

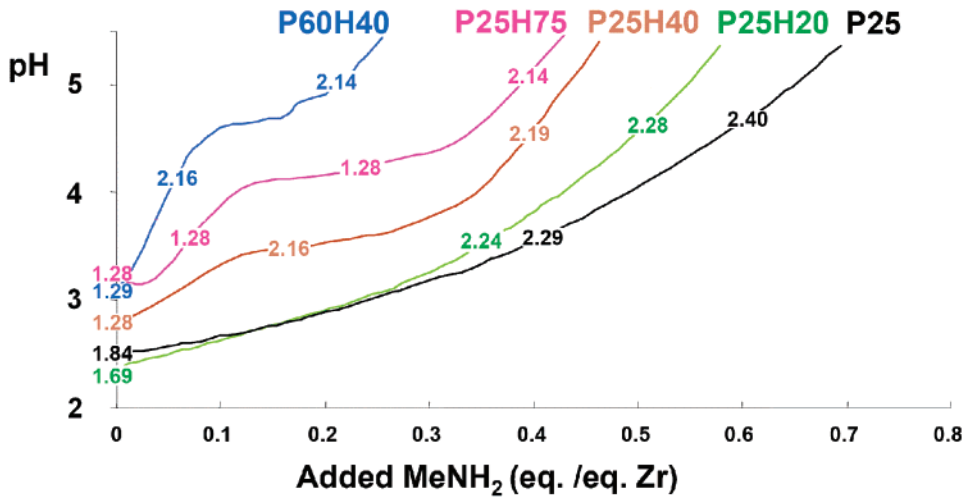

Figure 9. Titration curves of the indicated materials. Numbers on the graphs correspond to interlayer distances as measured by XRD on wet powders at the corresponding points of added $MeNH_2$.

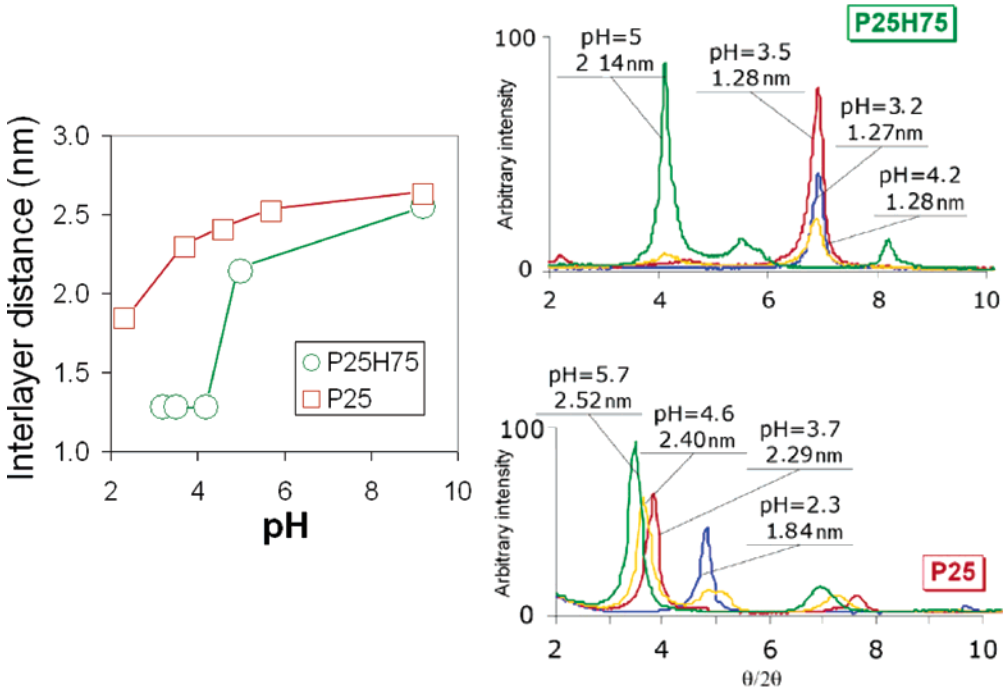

Figure 10. Variation of interlayer distance of the indicated materials with the pH (amount of added methylamine). The insets show expansions of the corresponding X-ray powder patterns at the indicated pH.

hypophosphite PH_2 bonds avoid phase swelling by the action of acid−base processes such as those taking place in the γ-ZrP intercalation of amines.

With these ideas in mind, we performed a comparative study of the behavior of **P25** and several of the created hypophosphite phases toward methylamine intercalation. Figure 9 contains the resulting titration curves. At regular intervals, the suspensions were centrifuged and the solid, wet material was taken to powder XRD to measure the interlayer distance, which is also included in Figure 9.

It may be seen for the starting **P25** that both the titration curve and the concomitant increase of its basal spacing (cf. Figure 9) are relatively smooth, suggesting a progressive diffusion of methylamine in the interlayer space. However, when hypophosphite is present, even at a fairly small level, several new events start to come about. First, the starting interlayer distance of the wet materials is much shorter (numbers at graph origin in Figure 9; cf. Table 2). **P25H20** and **P25H40** with 20% and 40% hypophosphite, respectively, hence still possessing a large amount of superficial acidic phosphate (55% and 35%, correspondingly), displayed interlayer spacings of 1.69 (green) and 1.28 nm (orange), respectively. The latter value appears to be the minimum possible because it is shared by **P25H75** (pink) and **P60H40** (blue), the studied materials with no left superficial phosphate. These are clear indications that the presence of the low polar hypophosphite makes the material highly hydrophobic, forcing the inorganic layers to be in the closest possible contact. In this situation, there should be little room for the organic chains that must squirm along the channels left by the rows of superficial hypophosphite groups.

The second important collection of events occurred when the addition of methylamine was started. While titration curves of **P25** and **P25H20** were very similar, the increment

of interlayer distance in the latter is more pronounced (0.45 and 0.55 nm, respectively, from 0 to ca. 0.4 equiv of added methylamine). For the rest of the materials, the higher the hypophosphite content, the steeper the initial ascend of the curve, which is followed by a plateau. This may be understood in terms of an initial accumulation of amine in the solution, which raises pH somewhat abruptly. The highly compressed microcrystals do not allow methylamine to diffuse into their interior. Yet, after ca. 0.1−0.15 equiv, the pH stabilizes, indicating that methylamine starts reacting steadily with the acidic groups of the solid phase. At this point, the interlayer distance suddenly changes from a highly compressed state (1.28 nm) to a extremely expanded one (2.1 nm) in a very narrow interval of added amine. Figure 10 summarizes these findings by comparing the swelling response of **P25** and **P25H75**.

In the case of the phase **P25H75** (and also **P25H40**), the hydrophobic forces governing the behavior of the γ-ZrPH phase should be still at work. The fact that their interlayer distances are very short and humidity independent (cf. Table 2) should be a manifestation of it. Yet, in the phases with high hypophosphite content, it should be noted that every organic phosphonate still possesses an acidic OH and hence reaction with the amine is possible, at least at the edges of every microcrystal. Had some methylamine molecules dared to get into the highly nonpolar interlayer region of these hypophosphite-rich solids, there should be few choices for the methylammonium ions to stabilize but forming tight ion pairs with the phosphonates. Consequently, the relatively bulky organic cations must rest very close to the organic chains acting as a wedge that they must force the pillars to stand up. Considering that the layers of the γ-ZrP phases are known to be very rigid, once a few amine molecules have diffused into the interlayer region close to its edges, the van der Waals forces are quickly disrupted and the layered material expands very quickly. The interlayer distance is then almost doubled in the very short interval of added amine of ca. 0.2 equiv. To the best of our knowledge, this enormous sensitivity of microcrystalline porosity toward intercalation of small molecules has no precedent so far.

Conclusion

This paper shows the versatility of the derivatives of γ-ZrP in that the inorganic salt can be easily pillared with appropriate organic moieties and doubly exchanged with other phosphorus functions, leading to a material whose pores can be controlled in size and polarity. The right choice of the organic part of the scaffold allows an aprioristic design of the solid material. Yet, more importantly, the final structure can be reversibly modified in the solid state, even in a drastic manner, by the simple intercalation of small molecules. We believe that the philosophy involved in this work, where the organization of the final microcrystalline material can be reasonably predicted from (i) the structure of its individual building blocks and (ii) the understanding of the interactions involved among them and with third-party species, constitutes a "solid" strategy to overcome Maddox's scandal.[36]

Acknowledgment. This paper is dedicated to Ernest L. Eliel on his 83rd birthday. This work was supported by MCYT of Spain under grants PB98-0103 and MAT2002-03243. We also thank FYSE-ERCROS S.A. (Aranjuez, Spain) for generous indirect funding. H.M.H.A. is grateful to the Spanish Cooperation Agency of the Ministry of Foreign Affairs for a fellowship. C.C. is thankful to the Ministry of Science and Education for an undergraduate fellowship.

Supporting Information Available: Synthetic procedures and spectroscopy data; complete data for Tables 1 and 2; sample TGA curve (PDF). This material is available free of charge via the Internet at http://pubs.acs.org.

CM048754Q

(36) One of the continuing scandals in the physical sciences is that it remains in general impossible to predict the structure of even the simplest crystalline solids from a knowledge of their chemical composition: Maddox, J. *Nature* **1988**, *335*, 201.